

PROTO-CLUSTERS IN THE Λ CDM UNIVERSE

TAMON SUWA¹, ASAO HABA², AND KOHJI YOSHIKAWA³

Draft version August 8, 2018

ABSTRACT

We compare the highly clustered populations of very high redshift galaxies with proto-clusters identified numerically in a standard Λ CDM universe ($\Omega_0 = 0.3$, $\lambda_0 = 0.7$) simulation. We evolve 256^3 dark matter particles in a comoving box of side $150h^{-1}\text{Mpc}$. By the present day there are 63 cluster sized objects of mass in excess of $10^{14}h^{-1}M_\odot$ in this box. We trace these clusters back to higher redshift finding that their progenitors at $z = 4-5$ are extended regions of typically 20–40 Mpc (comoving) in size, with dark halos of mass in excess of $10^{12}h^{-1}M_\odot$ and are overdense by typically 1.3–13 times the cosmological mean density. Comparison with the observation of Ly α emitting (LAEs) galaxies at $z = 4.86$ and at $z = 4.1$ indicates that the observed excess clustering is consistent with that expected for a proto-cluster region if LAEs typically correspond to massive dark halos of more than $10^{12}h^{-1}M_\odot$. We give a brief discussion on the relation between high redshift concentration of massive dark halos and present day rich clusters of galaxies.

Subject headings: galaxies:clusters:general – cosmology:theory – methods:numerical

1. INTRODUCTION

The formation and evolution of structures in the universe, such as galaxy clusters and large-scale structures, are part of the most important issue in astrophysics. Since clustering properties of galaxies in the distant universe give us great clues to this issue, many observations have been done in order to detect (proto) clusters of galaxies at high redshifts (Steidel et al. 1998, 2000; Campos et al. 1999; Pentericci et al. 2000; Rhoads et al. 2000; Ouchi et al. 2001, 2003; Miley et al. 2004). These deep surveys of galaxies, which have significantly advanced our understanding of the properties and distribution of galaxies at high redshifts, are equally important in constraining the underlying structure formation scenarios.

Venemans et al. (2002) showed a region around a radio galaxy in which number density of Ly α emitters (LAEs) is much higher than the mean of the universe suggested by Rhoads et al. (2000) at $z = 4.1$. The region has size of 2.7×1.8 Mpc (physical) and mass of $\sim 10^{15}M_\odot$. More recently, Shimasaku et al. (2003) found that LAEs are clustered in an elongated region with a size of 20×50 Mpc (comoving) at $z = 4.86$, which is comparable to the size of present-day large-scale structures. In this elongated region, there is a circular region of high surface density of LAEs with 12 Mpc radius, which may be a progenitor of a galaxy cluster. They also estimated the bias parameter of the LAEs in the range of $b \sim 3-16$ for spatially flat low-density cosmological model (Λ CDM model). The elongated distribution of the LAEs in this region is also proposed to be a part of large-scale structures, although observation by Shimasaku et al. (2004) of the same sky area which is closer to us by 39Mpc (comoving) does not show large structure. In addition, Hayashino et al. (2004) reported that LAEs distribution at $z = 3.1$ in their observed area shows broad large scale structure. They claim that this structure cannot be explained in the context of the standard CDM model.

Ouchi et al. (2005) observed LAEs at $z = 5.7$ and discovered filamentary structures and voids.

Although these regions which have much high number densities of LAEs are claimed to be proto-clusters, there is not yet enough detailed study on these possibilities. Therefore, we investigate formation and evolution of galaxy clusters in early universe using cosmological simulation. In this letter we report some properties of simulated proto-clusters at $z = 5$ and compare our numerical results with observations by Shimasaku et al. (2003) and Venemans et al. (2002).

2. METHOD

2.1. Numerical Method

We perform a cosmological N-body simulation with Particle-Particle-Particle-Mesh (P³M) algorithm (Hockney & Eastwood 1981). Our simulation code is the same one which was used in Yoshikawa, Jing, & Suto (2000). We use the following values as parameters of our simulation: the Hubble constant in units of $100\text{km s}^{-1} \text{Mpc}^{-1}$, $h = 0.7$, the density parameter, $\Omega_0 = 0.3$, the baryon density parameter, $\Omega_b = 0.015h^{-2}$, the root mean square density fluctuation amplitude on a scale $8h^{-1}\text{Mpc}$, $\sigma_8 = 1.0$, the power-law index of the primordial density fluctuation, $n = 1.0$, and the cosmological constant parameter, $\lambda_0 = 0.7$. We employ $N_{\text{DM}} = 256^3$ dark matter particles and the mass of each one is $2.15 \times 10^{10}M_\odot$. The size of the comoving simulation box, L_{box} , is $150h^{-1}\text{Mpc}$, and the box is on the periodic boundary condition. This size of the box is large enough to realize a sufficient number of clusters and large-scale structures at $z = 0$. We use the spline (S2) softening function for gravitational softening, and the softening length, ϵ_{grav} , is set to be $L_{\text{box}}/(10N_{\text{DM}}^{1/3})$ ($\sim 60h^{-1}\text{kpc}$ in the comoving scale).

2.2. Identification of Dark Halos and Proto-clusters

We identify dark halos in a manner similar to that of Suwa et al. (2003). A brief explanation of the identification is as follows: First, we define densities of dark matter particles using an interpolation technique in the same way of the Smoothed Particle Hydrodynamics method (Monaghan 1992), and pick up particles whose densities are more than

arXiv:astro-ph/0606292v2 15 Jun 2006

¹ Center for Computational Sciences, University of Tsukuba, Tsukuba 305-8577, Japan; tamon@ccs.tsukuba.ac.jp

² Division of Physics, Graduate School of Science, Hokkaido University, Sapporo 060-0810, Japan; habe@astro1.sci.hokudai.ac.jp

³ Department of Physics, School of Science, The University of Tokyo, 7-3-1 Hongo, Bunkyo-ku, Tokyo 113-0033, Japan; kohji@utap.phys.s.u-tokyo.ac.jp

the virial density. Next, we perform the hierarchical friends-of-friends (HFOF) method (Klypin et al. 1999) for the selected dense particles. The maximum linking length l_{\max} in HFOF method is defined as $0.2\bar{l}$, where \bar{l} is the mean inter-particle distance for all (not only dense) particles. Then we draw a sphere of which the center is on the densest particle of the group and seek the radius in which the mean density of total matter is equal to the virial density. We regard the set of particles in the sphere as a virialized object. If a centroid of a sphere exists in another sphere, only the set which belongs to the more massive sphere is used. We regard dark halos which have mass of more than $10^{14}h^{-1}M_{\odot}$ at $z=0$ as galaxy clusters and we analyze properties of their progenitors to compare with the observations of proto-cluster regions (Venemans et al. 2002; Shimasaku et al. 2003).

We seek proto-clusters in high redshift universe as follows: First, we pick up all particles in each cluster at $z=0$. Next, we trace those particles back to high- z epoch, e.g. $z=5$. Finally, we set a minimum cubic region which covers all of the particles. We call the region as ‘‘proto-cluster region’’ for the cluster. This region contains the proto-cluster of the present cluster.

In order to investigate galaxy distribution in the proto-cluster regions, we identify galaxy-size dark halos ($M > 10^{12}h^{-1}M_{\odot}$) in the regions at $z=5$. Dark halos of this mass scale are suggested to contain LAEs and LBGs from their spatial distribution arguments (Hamana et al. 2004).

2.3. Overdensity

In proto-cluster regions, it is expected that dark halos which correspond to galaxies concentrate much denser than the background. Therefore the excess of number density of dark halos, δ_{halo} , should be useful quantities to compare the result of the simulation to observations:

$$\delta_{\text{halo}} = \frac{\bar{n}_{\text{halo}}}{n_{\text{halo,BG}}} - 1, \quad (1)$$

where \bar{n}_{halo} is the halo number density averaged in the suitable scale (e.g. 25 Mpc) and $n_{\text{halo,BG}}$ is the background halo number density.

The mass overdensity, δ_{mass} , is defined in a similar way:

$$\delta_{\text{mass}} = \frac{\rho}{\rho_{\text{BG}}} - 1, \quad (2)$$

where ρ is the density of the region under consideration and ρ_{BG} is that of the background. The combination of the halo overdensity and the mass overdensity give us important information of mass concentration, so-called bias information, which has been investigated in analytical and numerical works (e.g. Kaiser 1984; Taruya & Suto 2000; Yoshikawa et al. 2001).

3. RESULTS

We find 63 galaxy clusters with $M > 10^{14}h^{-1}M_{\odot}$ in the simulation box at the present epoch ($z=0$). We seek their progenitors, i.e. proto-clusters, in high redshift universe and study their properties. We show an example of present galaxy clusters and proto-cluster regions in our simulation box at $z=5$ in Figure 1.

In our numerical results, the size of the proto-cluster regions is in the range of 20–40Mpc in the comoving scale. The extension is similar to that of the LAEs dense region observed by Shimasaku et al. (2003). Several dark halos with $M > 10^{12}h^{-1}M_{\odot}$ already exist in proto-cluster regions at $z=5$

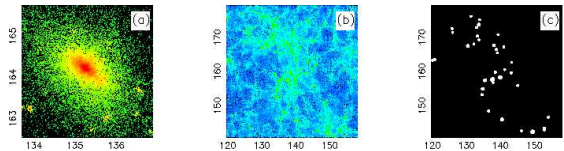


FIG. 1.— Distributions of dark matter and dark halos in an example cluster and the corresponding proto-cluster region in the simulation box. Panel (a) and (b) show the distribution of dark matter at $z=0$ and $z=5$, respectively. Panel (c) shows the distribution of dark halos which have mass of more than $10^{12}h^{-1}M_{\odot}$ in the proto-cluster region shown in the panel (b). x - and y -axes are comoving position coordinate in the simulation.

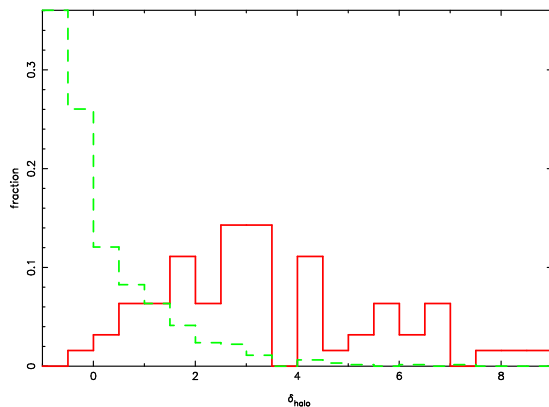


FIG. 2.— Histogram of halo number overdensities, δ_{halo} , of the proto-cluster regions (red solid line) and the randomly selected region (green dashed line) at $z=5$.

as shown in Figure 1(c). We obtain bulk velocity of each dark halo in the proto-cluster regions and found that dispersion of those are typically $\sim 200\text{km s}^{-1}$.

We calculate δ_{halo} and δ_{mass} for each proto-cluster regions at $z=5$, by assuming a smoothing scale of 25 Mpc (comoving) that is a typical proto-cluster size in our numerical results. In order to show that the values of these indicators have significant excess than the mean value of the universe, we randomly select $(25\text{Mpc})^3$ regions in the simulation box and calculate δ_{halo} and δ_{mass} for these regions. The number of the randomly selected regions is 630, which is 10 times more numerous than the proto-cluster regions. We show the histograms of δ_{halo} in Figure 2, where the red solid line is for the proto-cluster regions and the green dashed line is for the randomly selected regions. The red solid line is significantly different from the green dashed line. Figure 2 shows that the typical value of δ_{halo} is ~ 3 for the proto-cluster regions, and its variance is very large. On the other hand, δ_{halo} in most of the randomly selected regions are almost -1 , where this value means that there is no massive dark halo in the regions.

The mass overdensities, δ_{mass} , for the proto-cluster regions are clearly different from the randomly selected regions as shown in Figure 3. δ_{mass} of the proto-cluster regions are in the range of 0.2–0.4, while those of the randomly selected regions range from -0.2 to 0.2. The typical value of δ_{mass} of the proto-cluster regions is ~ 0.4 and the variance of δ_{mass} is much smaller than that of δ_{halo} .

In order to show the bias of dark matter halo distribution in the proto-cluster regions, we plot δ_{mass} and δ_{halo} for the proto-cluster regions and the randomly selected regions in Figure 4. Red triangles, blue crosses, and green squares indicate the proto-cluster regions, the randomly selected regions which overlap more than 50% with some proto-cluster region, and

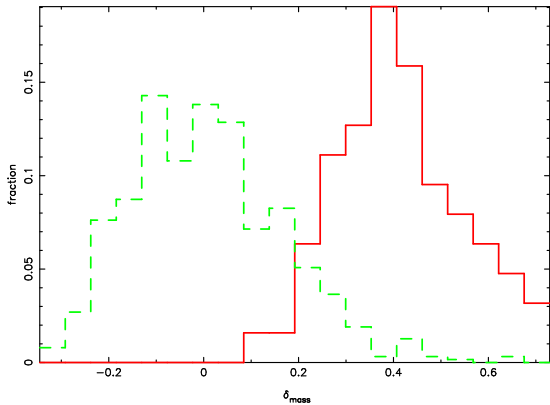
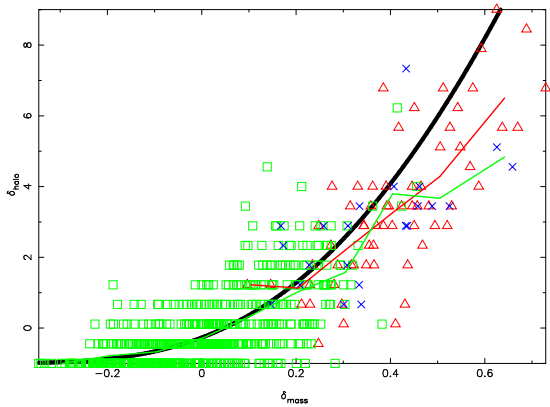
FIG. 3.— Same as Figure 2, but for δ_{mass} .

FIG. 4.— Correlation map of δ_{mass} and δ_{halo} . Red triangles, blue crosses, and green squares indicate the proto-cluster regions, the randomly selected regions which overlap more than 50% with some proto-cluster region, and other randomly selected regions, respectively. The analytical relation is indicated by a thick black line. Green and red lines are correspond to average value of simulated regions randomly selected (both field and overlapped) and proto-clusters, respectively.

other randomly selected regions, respectively. Figure 4 shows correlation between the values of δ_{halo} and δ_{mass} for $\delta_{\text{mass}} > 0$, although the dispersion is very large. It is clear that the regions with large δ_{mass} have large δ_{halo} . This relation corresponds to the bias of dark matter halo distribution in the proto-cluster regions.

We compare the $\delta_{\text{mass}}-\delta_{\text{halo}}$ relation in our numerical results with the analytical result given by the natural bias theory (Mo & White 1996) in Figure 4. In Figure 4, we show the analytical relation by a thick black line, where we use the Press-Schechter mass function formula and the relation of linear extrapolation to nonlinear evolution for density perturbation (Carroll, Press, & Turner 1992). Green and red lines in Figure 4 indicate average value of the randomly selected regions and the proto-clusters, respectively. The relation between the $\delta_{\text{mass}}-\delta_{\text{halo}}$ given by the natural bias theory agrees well with our numerical results as shown in Figure 4, except for gradual deviation $\delta_{\text{mass}} > 0.4$. This deviation may be explained by the effect of limitation of our simulation box size. Our simulation box size is not enough to consider large-scale ($100h^{-1}\text{Mpc}$) component of density fluctuation and this limitation may cause underestimation of mass function for $10^{12}M_{\odot}$ dark halos at $z = 5$ (Bagla & Ray 2005).

It is very important to show a critical value of δ_{halo} , $\delta_{\text{halo,c}}$,

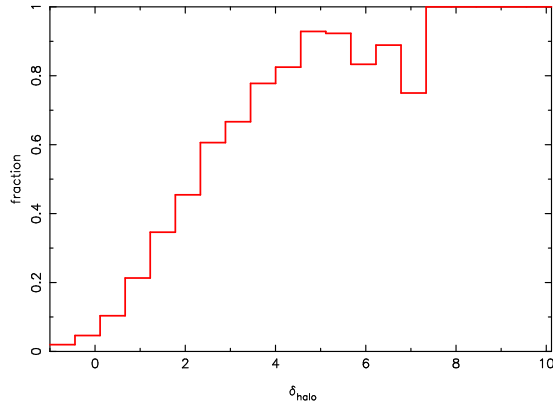


FIG. 5.— Fraction of randomly selected cubic regions which contain a galaxy cluster at $z = 0$ as a functions of δ_{halo} at $z = 5$. The size of the cubic regions is 25 Mpc (comoving).

by which we can select a proto-cluster region. In order to search $\delta_{\text{halo,c}}$, we compare values of halo overdensity, δ_{halo} , in the randomly selected regions at $z = 5$ and masses of the largest dark halos in the regions at the present epoch. Figure 5 shows a fraction of the regions which contain galaxy clusters with $M > 10^{14}h^{-1}M_{\odot}$ at $z = 0$ as a function of δ_{halo} at $z = 5$. It is clear in Figure 5 that most regions with $\delta_{\text{halo}} \geq 3$ at $z = 5$ will evolve rich clusters with mass of more than $10^{14}h^{-1}M_{\odot}$ at $z = 0$.

4. DISCUSSION

We have investigated proto-cluster regions and the difference between those regions and background field regions using N-body cosmological code. In order to investigate proto-clusters, we identify 63 galaxy clusters at in our cosmological simulation $z = 0$, and trace dark matter particles which belong to those, back to a high redshift epoch. We study properties of the proto-cluster regions by analyzing the mass overdensity, δ_{mass} , and the halo overdensity, δ_{halo} , of which definitions are given in §2. The results at $z = 5$ are shown in Figures 2, 3, and 4. As expected from the bias theory (e.g. Taruya & Suto 2000), δ_{halo} shows excess over δ_{mass} and variance of δ_{halo} is much larger than that of δ_{mass} .

In order to show difference between the proto-cluster regions and the field, we calculate δ_{mass} and δ_{halo} for the randomly selected regions with the same size of the typical proto-cluster region at $z = 5$ (25 Mpc in the comoving scale). We select 630 regions (10 times greater than the proto-cluster regions) for the randomly selected regions. Clustering properties of the dark halos in these regions are significantly different from those in the proto-cluster regions. The halo overdensities for most of the randomly selected regions are much smaller than those for the proto-cluster regions as shown in Figure 2.

It is very interesting to study a critical value of δ_{halo} by which we can select a region as the proto-cluster regions. From Figure 5, we have found that more than 80% of the regions with $\delta_{\text{halo}} \geq 3$ at $z = 5$ contain rich clusters ($M \geq 10^{14}h^{-1}M_{\odot}$) at the present epoch. Thus, we conclude that $\delta_{\text{halo}} \geq 3$ is a good criterion to distinguish proto-cluster regions from field regions at $z = 5$. This criterion is very useful to judge whether observed galaxies excess regions are actual proto-clusters or not.

It should be pointed out that there are a few regions which do not contain clusters at $z = 0$ but have large δ_{halo} values

(3–7) at $z = 5$, although a fraction of those regions are very small. We discuss that the physical origin of the large δ_{halo} is non-linearity and stochasticity of bias parameters proposed by Taruya & Suto (2000). They studied variance of biasing parameters, and conclude that the variance increases strongly with redshift. They also conclude that stochasticity of the biasing is generated by the scatter in the halo mass distribution at higher redshift. Yoshikawa et al. (2001) confirmed these results for $0 < z < 3$ by large P³M simulation. We conclude that our results for $z = 3$ are consistent with their results and the trend of evolution of bias variance is still true for $3 < z < 5$.

We compare our results with the observation of Shimasaku et al. (2003). Properties of the LAEs concentrated region reported by them are as follows: (1) Diameter of the region is 25 Mpc (comoving unit), (2) Projected overdensity of LAEs $\delta_{\Sigma} \sim 2$, (3) Bias parameter is estimated 3–16 for Λ CDM model, and the best-fit value is $b \sim 6$, i.e. $\delta_{\text{mass}} \sim 0.3$. (4) The number of LAEs in the region is about 20. Properties from (1) to (3) are consistent with our numerical results of proto-cluster regions, if LAEs correspond to dark halos with mass more than $10^{12}h^{-1}M_{\odot}$, which is suggested by Hamana et al. (2004) using correlation function on small-scales. The typical number of dark halos in the simulated proto-clusters is 5–10, which is about half of that of observed LAEs. One explanation of this discrepancy is due to possibility that some dark halos have more than one

LAEs. We speculate that some pairs of LAEs in Fig. 3 of Shimasaku et al. (2003) are included in the same dark halo. It is also possible that some of observed sample of LAEs in the region are low redshift interlopers. Shimasaku et al. (2003) estimate the contamination of their sample to be about 20%.

Venemans et al. (2002) also reported properties of a LAEs rich region. The size of the region is $\sim 14 \times 10$ Mpc (comoving unit). They estimate the region is overdense in LAEs by a factor of 15 compared with the blank field (Rhoads et al. 2000). The overdensity is much larger than that of proto-clusters at $z = 4$ in our simulation and the size of their observed region is smaller than the typical size of the proto-clusters in our simulation. Therefore, we suggest that the region observed by them is not a whole proto-cluster region, but the central region of the proto-cluster because of small size of the observed region and their high value of the overdensity.

We would like to thank Prof. Masayuki Fujimoto and Dr. Takayuki Saitoh for helpful advice, insightful discussions and encouragement. We are also grateful to Prof. Tom Broadhurst for useful comments. Numerical computations in this work were carried out on SGI Onyx300 in the Hokkaido University Computing Center by parallel computation with 16 CPUs.

REFERENCES

- Bagla, J. S., & Ray, S. 2005, MNRAS, 358, 1076
 Campos, A., Yahil, A., Windhorst, R. A., Richards, E. A., Pascarelle, S., Impey, C., & Petry, C. 1999, ApJ, 511, L1
 Carroll, S. M., Press, W. H., & Turner, E. L. 1992, ARA&A, 30, 499
 Hamana, T., Ouchi, M., Shimasaku, K., Kayo, I., & Suto, Y. 2004, MNRAS, 347, 813
 Hayashino, T. et al. 2004, AJ, 128, 2073
 Hockney, R. W. & Eastwood, J. W. 1981, Computer Simulation Using Particles (New York: McGraw-Hill)
 Kaiser, N. 1984, ApJ, 284, L9
 Klypin, A., Gottlöber, S., Kravtsov, A. V., & Khokhlov, A. M. 1999, ApJ, 516, 530
 Miley, G. K. et al. 2004, Nature, 427, 47
 Mo, H. J. & White, S. D. M. 1996, MNRAS, 282, 347
 Monaghan, J. J. 1992, ARA&A, 30, 543
 Ouchi, M. et al. 2001, ApJ, 558, L83
 —. 2003, ApJ, 582, 60
 —. 2005, ApJ, 620, L1
 Pentericci, L. et al. 2000, A&A, 361, L25
 Rhoads, J. E., Malhotra, S., Dey, A., Stern, D., Spinrad, H., & Jannuzi, B. T. 2000, ApJ, 545, L85
 Shimasaku, K. et al. 2003, ApJ, 586, L111
 —. 2004, ApJ, 605, L93
 Steidel, C. C., Adelberger, K. L., Dickinson, M., Giavalisco, M., Pettini, M., & Kellogg, M. 1998, ApJ, 492, 428
 Steidel, C. C., Adelberger, K. L., Shapley, A. E., Pettini, M., Dickinson, M., & Giavalisco, M. 2000, ApJ, 532, 170
 Suwa, T., Habe, A., Yoshikawa, K., & Okamoto, T. 2003, ApJ, 588, 7
 Taruya, A. & Suto, Y. 2000, ApJ, 542, 559
 Venemans, B. P. et al. 2002, ApJ, 569, L11
 Yoshikawa, K., Jing, Y. P., & Suto, Y. 2000, ApJ, 535, 593
 Yoshikawa, K., Taruya, A., Jing, Y. P., & Suto, Y. 2001, ApJ, 558, 520